Equilibrium Segment Density Distribution of a Diblock Copolymer Segregated to a Polymer/Polymer Interface

Kevin H. Dai, Laura J. Norton, and Edward J. Kramer*

Department of Materials Science and Engineering and the Materials Science Center, Cornell University, Ithaca, New York 14853

*Received September 2, 1993; Revised Manuscript Received December 11, 1993**

ABSTRACT: Utilizing neutron reflectometry, we have determined the segment density (volume fraction) profiles of the deuteriopolystyrene (dPS) block of a diblock copolymer of poly(styrene-d_8-*b*-2-vinylpyridine) (dPS–PVP) segregating to the interface between the homopolymers PS and PVP as a function of ϕ_∞, the volume fraction of diblock copolymer remaining in the host homopolymer after annealing the specimens to reach the equilibrium segregation. These segment density profiles were used to determine the interfacial excess (z^*_i), which was found to be in good agreement with direct measurements of z^*_i using forward recoil spectrometry. The interaction parameter $\chi_{PS\text{-}PVP}$ was established from the best fit of a self-consistent mean field (SCMF) theory to the measured segregation isotherm, i.e., z^*_i versus ϕ_∞. With this $\chi_{PS\text{-}PVP}$, the SCMF theory can reproduce the experimental volume fraction profile of the dPS block accurately except very close to the interface; the measured profile is broader at the interface as compared to the predicted profile. This excess broadening is observed for all ϕ_∞'s and tends to be enhanced as z^*_i increases. We believe that most of the interface broadening is due to the "roughening" of the equilibrium interface encouraged by the decrease in interfacial tension accompanying the copolymer segregation. Excellent agreement between the measured profiles and the theoretical predictions of SCMF theory at various ϕ_∞'s is found if a Gaussian convolution is used to represent the effect of the interfacial roughness.

Introduction

Adhesion between polymers strongly depends on the interpenetration of molecules at the interface. Such interpenetration creates entanglements between molecules from different polymer phases, which, in turn, increase the entanglement density across the interface, thus increasing the adhesion between the two phases. The interface formed between strongly immiscible polymers is fairly sharp, and only a small extent of interpenetration of molecules is allowed due to the highly unfavorable enthalpic interaction between the two chemically different polymers. Therefore, reinforcement of such an interface becomes an important subject in designing polymer materials such as phase-separated blends. ABS plastic is a typical example employing interfacial reaction between two phases, so-called grafting, to reinforce the interface: butadiene rubber forms second-phase particles in a matrix of styrene–acrylonitrile copolymer and then the reaction between styrene–acrylonitrile copolymer and butadiene rubber ensures a good adhesion at the interface between the rubber and glassy phases.[1] Such modification via chemical reaction (grafting) requires efforts to match the particular combination of polymer components. In contrast, a modification method without involving chemical reactions may be more generally applicable. Improved adhesion[2-5] has been achieved by physical segregation of block copolymers to the interface where each block stretches into its respective homopolymer, forming entanglements with polymer chains from both phases. Such entanglements and the covalent joints between copolymer blocks effectively increase the entanglement density across the interface to improve the adhesion. In addition to mechanical reinforcement of an interface, the reduction in interfacial tension due to the segregation[6] can be utilized to regulate the particle size so as to optimize the properties of a phase-separated polymer blend.[7-9] Therefore, the distribution of copolymer segments at the interface plays a very important role in such applications. Knowledge of this segment distribution provides insight into the thermodynamics of segregation as well as understanding of the interfacial modification via segregation on a molecular scale. Neutron reflectometry (NR) with its excellent depth resolution of 5–10 Å provides an excellent tool to reveal the detailed segment distribution.[10]

A qualitative approach proposed by Leibler[11] provides a basic understanding of the copolymer segregation at polymer–polymer interfaces. In general, the enthalpic interaction between components dominates the phase behavior in polymer blends. The mixing free energy of an A–B copolymer chain in homopolymer A mostly comes from the unfavorable interaction between B segments of the copolymer and A segments of the homopolymer as represented by the Flory interaction parameter χ. The portion of the chemical potential resulting from this enthalpic interaction is what drives the copolymer to segregate to the polymer–polymer interface. Based on Leibler's scheme, this unfavorable interaction is simply minimized by confining the copolymer joints at the interface at the expense of an entropy loss due to the chain localization and an increase in elastic free energy due to the stretching of the copolymer chain at the interface. As shown previously,[12,13] this simple argument can indeed reproduce the form of the segregation isotherm, namely, the interfacial excess z^*_i versus the volume fraction ϕ_∞ of copolymer in the host homopolymer phase far from the interface if the Flory interaction parameter χ is treated as an adjustable fitting parameter. However, different values of χ are necessary to reproduce the observed segregation isotherms if the molecular weights of the homopolymers are varied.[12] Recently, Semenov[14] proposed a model which reconciles the fact that the copolymer joints are not strictly confined at the interface. Although this model produces an isotherm in good agreement with the observed isotherm using an appropriate χ if the molecular weight of homopolymer is relatively high, it still fails to account for the dependence of segregation on the molecular weights of homopolymers.

* Abstract published in *Advance ACS Abstracts*, February 1, 1994.

0024-9297/94/2227-1949$04.50/0

The first self-consistent mean field (SCMF) theory for the homopolymer interface with no block copolymer additive was developed by Helfand and Tagami[15] for the strong segregation limit. This approach was then adopted by Hong and Noolandi[16,17] to describe the case of block copolymer segregation at an immiscible homopolymer interface in the presence of a solvent and further adapted to describe the solvent-free case by Shull and Kramer.[18] As in Leibler's and Semenov's models, the Flory interaction parameter χ remains as an adjustable parameter in the SCMF theory. However, only the SCMF theory can reproduce the segregation isotherm with a single value of χ when the molecular weights of homopolymers are varied.[12] To further check these theories, we examine in this paper the segment density profile of the copolymer component using a high-resolution technique, neutron reflectometry, and compare the results with the theoretical predictions.

Recently, Russell et al.[19] reported a study of the segment density distribution of a symmetric diblock copolymer at the interface between homopolymers by neutral reflectometry. This experiment clearly demonstrates the capability of NR to reveal the density distribution of each polymer component. However, their experiment was performed by placing a layer of the diblock copolymer between two homopolymer layers prior to annealing. Given the long symmetric diblock copolymer used, it seems likely that the segment density distribution was a result of a nonequilibrium "trapping" of copolymer at the interface. Although the experiments of Russell et al. provide useful information on the distribution of copolymer blocks under their special conditions, no connection to the thermodynamics of segregation can be drawn, especially because the concentration of their diblock copolymer away from the interface was too small for them to measure and thus made it impossible to define the chemical potential of the copolymer in the bulk homopolymer phase. It is very important to point out that our experiments have been conducted with a diblock copolymer designed so that this bulk concentration is measurable. Furthermore, under our annealing conditions, the diblock copolymer at the interface is believed to be in equilibrium with that in the bulk phase.

Experimental Section

Materials. A diblock copolymer, poly(styrene-d_8-*b*-2-vinylpyridine) (dPS–PVP), was synthesized by anionic polymerization with cumylpotassium as the initiator. A small amount of dPS precursor was sampled from the reactor prior to the addition of 2-vinylpyridine monomer. Using this precursor, we determined the degree of polymerization of the dPS block to be 597 by size exclusion chromatography (SEC). Forward recoil spectrometry (FRES) and ^{13}C NMR were then used to evaluate the molar ratio between dPS and PVP, which yields a degree of polymerization for the PVP block of 59. The polydispersity index of the resulting block copolymer is <1.1, as determined by SEC. The homopolymer PVP was synthesized by procedures similar to those used to prepare the block copolymer. The degree of polymerization and polydispersity index of the PVP homopolymer are ~2000 and 1.2, respectively, determined by SEC with PS standards as the reference. PS and dPS homopolymers of molecular weights of 233K and 105K, respectively, with polydispersity <1.1 were purchased from Polysciences, Inc., and used as received.

Polished silicon wafers (5 cm in diameter and 0.47 cm thick) were used as substrates. Wafers were first cleaned by reactive ion etching (RIE) using an oxygen plasma and then placed into buffered HF solution (pH = 5–6) to remove the native oxide layer. The stripped silicon substrates were rinsed thoroughly with deionized water, and the water droplets on the surface were then removed by a blast of dry nitrogen. The purpose of stripping off the oxide layer is to eliminate the complication of data analysis caused by an additional layer of high neutron scattering length density. The stripped silicon wafer was immediately coated with a layer of PVP homopolymer from acetic acid (glacial acetic acid) via spin-casting. This PVP-coated substrate was then dried in the air at room temperature.[20]

The block copolymer dPS–PVP was blended with PS homopolymer in various concentrations, leading to ϕ_∞ ranging from 0.004 to 0.048, where ϕ_∞ is the copolymer volume fraction remaining in the host PS homopolymer after annealing the specimen to reach the equilibrium segregation. It is to be pointed out that the copolymer is asymmetric with a PVP fraction of 9% and the molecular weights of both homopolymers are at least 3 times larger than those of their respective copolymer components. These blends were spun-cast onto the PVP-coated substrates from toluene, which does not swell PVP strongly. These bilayer specimens were then annealed at 178 °C in vacuum for at least 12 h. No further segregation of the copolymer to the interface was detected by FRES, with longer annealing showing that the equilibrium had been reached. This conclusion has been further bolstered by recent experiments in which reversible segregation of this block copolymer to and from the interface with changes in annealing temperature has been demonstrated.[21] A bilayer specimen of dPS homopolymer coated onto a PVP substrate was prepared to examine the homopolymer/homopolymer interface for the case in which no block copolymer is added to the homopolymer.

Neutron Reflectivity Observation. Neutron reflectometry (NR) was used to probe the segment density profile at the interface between PS and PVP homopolymers as a function of ϕ_∞. The NR experiments were performed on the POSYII beam line at the Intense Pulsed Neutron Source (IPNS) of the Argonne National Laboratory. Neutrons are generated upon impingement of a pulsed proton beam on a uranium target. The resulting incident neutrons possess a distribution of wavelength λ from 2.5 to 15 Å, peaked at 4 Å. The principles and the procedures of NR are briefly summarized in what follows; further details can be found in a recent review article.[10] The reflectivity (R) of the sample for neutrons is measured as a function of k_z, the perpendicular component of the incident wave vector defined as $k_z \equiv (2\pi/\lambda)\sin\theta$. Different incident angles θ are used to achieve overlapping ranges of k_z up to approximately 0.05 Å^{-1}. $R(k_z)$ is determined by the neutron scattering length density (b/V) profile of the specimen in the direction (z) normal to the interface. Selective isotope substitution of hydrogen by deuterium provides sufficient contrast to isolate the segment density profile of the deuterated PS block of the block copolymer. A standard multilayer algorithm[22] and an assumed neutron scattering length density profile approximated by a series of uniform layers were used to calculate the reflectivity; the number of layers was chosen to be large enough so that no difference in the calculated reflectivity is observed as a finer mesh is used. This calculated reflectivity is then compared with the measured reflectivity, and this procedure is repeated until good agreement between the calculated and the measured reflectivities is reached. The final profile from this fitting procedure may be checked for consistency: the overall volume fraction of copolymer as well as the interfacial excess z^*_i may be calculated from the dPS segment density profile and compared to the actual volume fraction and the interfacial excess measured independently by forward recoil spectrometry.

Results and Discussion

Since the reflectivity of a single sharp interface (the Fresnel reflectivity) decays as k_z^{-4} for large k_z, a plot of Rk_z^4 as a function of k_z is a useful way to present the neutron reflectivity data. Figure 1 shows the reflectivity data plotted in this way for the bare homopolymer–homopolymer interface. Because the relative angular divergence ($\Delta k_z/k_z$) of the incident neutrons varies somewhat with incident angle, the reflectivity data from different incident angles cannot be superposed and are plotted separately. The inset in Figure 1, and in the subsequent figures, represents the neutron scattering

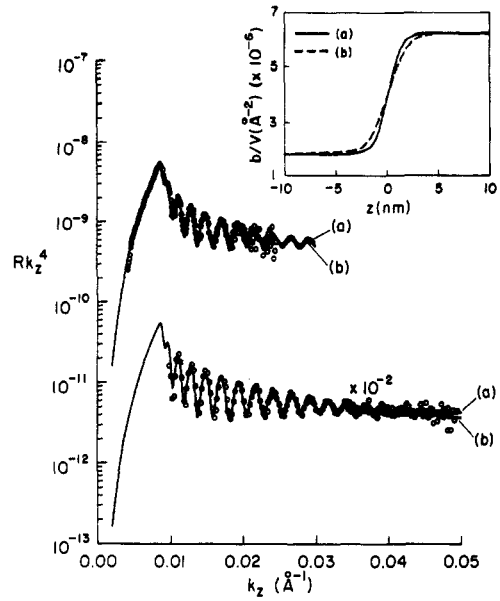

Figure 1. Neutron reflectivity data for a bilayer specimen of dPS and PVP; no block copolymer is added. In this figure, as in the remaining figures, different sets of data are obtained for different incident angles; the circles represent the experimental data; the solid line represents the calculated reflectivity using the (b/V) profile shown in the inset.

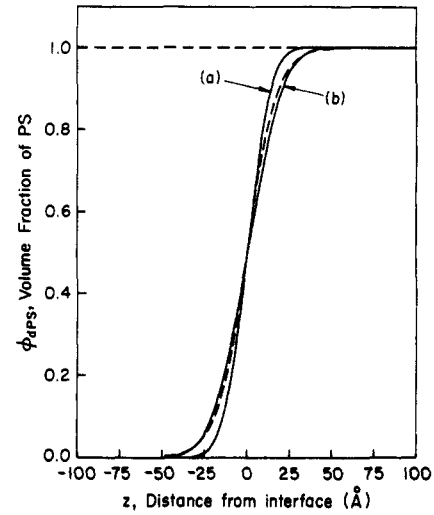

Figure 2. Volume fraction versus depth profiles of the dPS homopolymer, $\phi_{dPS}(z)$, converted from the corresponding (b/V) profiles shown in the inset of Figure 1 for the bilayer specimen of dPS and PVP. The dashed line is a tanh function (eq 1) with w = 34 Å.

length density (b/V) profile used to generate the specific (best) fit to the reflectivity data shown as the solid line in which a different $\Delta k_z/k_z$ is used for each incident angle. The surface roughness used in the reflectivity calculation is 5–7 Å in all cases, which is known to be a typical roughness of a spun-cast polymer film on a silicon wafer.[23] The overall scattering length density, $(b/V)_{total}$, is calculated by summing the scattering length density of each component weighted by its volume fraction. Thus for a two-component system (e.g., in the case of the bare homopolymer–homopolymer interface), the (b/V) profile can be converted directly into a volume fraction profile unambiguously. The solid lines shown in Figure 2 represent the volume fraction profile determined from the corresponding (b/V) profiles in the inset of Figure 1. The scattering length densities for the polymers relevant to this study are given in Table 1. As seen in Figure 1, these two volume fraction profiles with two quite different

Table 1. Neutron Scattering Length Density

polymer	$(b/V)^a$ (×10⁻⁶ Å⁻²)
dPS[b]	6.2
hPS	1.4
PVP	1.8

[a] Corresponding to bulk density. [b] 94% deuteration.

interfacial widths, as defined in eq 1, of ~27 and 40 Å produce nearly the same good fit to the reflectivity data.

$$w = \left(\frac{\partial \phi_{dPS}(z)}{\partial z}\right)^{-1}_{\phi_{dPS}=0.5} \tag{1}$$

The functional form of hyperbolic tangent was derived by Helfand and Tagami[24] to describe the segment density profile at the interface between strongly immiscible homopolymers with infinite molecular weights, viz.

$$\phi_{dPS}(z) = \frac{1}{2}\left[1 + \tanh\left(\frac{2(z - z_0)}{w}\right)\right] \tag{2}$$

where w is a measure of interfacial width as defined in eq 1 and z_0 is an offset of the interface from the surface. As shown in Figure 2, the tanh volume fraction profile with an effective width $w \sim 34$ Å demonstrates a good fit to the profile measured by NR. The theoretical interfacial width for highly immiscible polymers is given by eq 3:[24]

$$w = \frac{2a}{(6\chi)^{1/2}}\left[1 + \frac{\ln 2}{\chi}\left(\frac{1}{P_{hPS}} + \frac{1}{P_{hPVP}}\right)\right] \tag{3}$$

where a (=6.7 Å for PS;[26] we assume a = 6.7 Å for PVP as well) and χ (=0.105[12,21,27]) are the statistical length of the polymers and the Flory interaction parameter between PS and PVP, respectively. The parameters P_{hPS} and P_{hPVP} are the degrees of polymerization of homopolymers PS and PVP, respectively. The predicted interfacial width is 16.6 Å, which is significantly less than the measured value 30 Å. This discrepancy may be caused by the apparent roughness of the interface, which smears the interfacial density profile and, in turn, leads to a broadening of the interfacial width; this possibility will be discussed in greater detail below.

For the case in which block copolymer is added to the film bilayer and interface, the overall scattering length density (b/V) can be written explicitly as follows:

$$\frac{b}{V} = \phi_{dPS}\left(\frac{b}{V}\right)_{dPS} + \phi_{PVP}\left(\frac{b}{V}\right)_{PVP} + \phi_{hPS}\left(\frac{b}{V}\right)_{hPS} + \phi_{hPVP}\left(\frac{b}{V}\right)_{PVP} \tag{4}$$

The (b/V) as a function of depth ($(b/V)_z$) is experimentally measured, and the scattering length densities of the polymer components are given in Table 1. In general, by combining eq 4 with the constraint that $\sum\phi_i = 1$, where subscript i represents each component, one can construct two independent equations. In addition, another independent equation can be derived based on the fact that ϕ_{dPS}/ϕ_{PVP} far away from the interface is equal to N_{dPS}/N_{PVP} according to the condition of homogeneous mixing between the block copolymer and the homopolymer in the bulk phase. Nevertheless, in eq 4 the number of unknowns (i.e., 4) is more than the number of independent equations. Hence, one has to make reasonable approximations to impose constraints to reduce the number of unknown variables to render the equations solvable. The details of the procedures used for converting a (b/V) profile to a $\phi_{dPS}(z)$ profile are given in the Appendix.

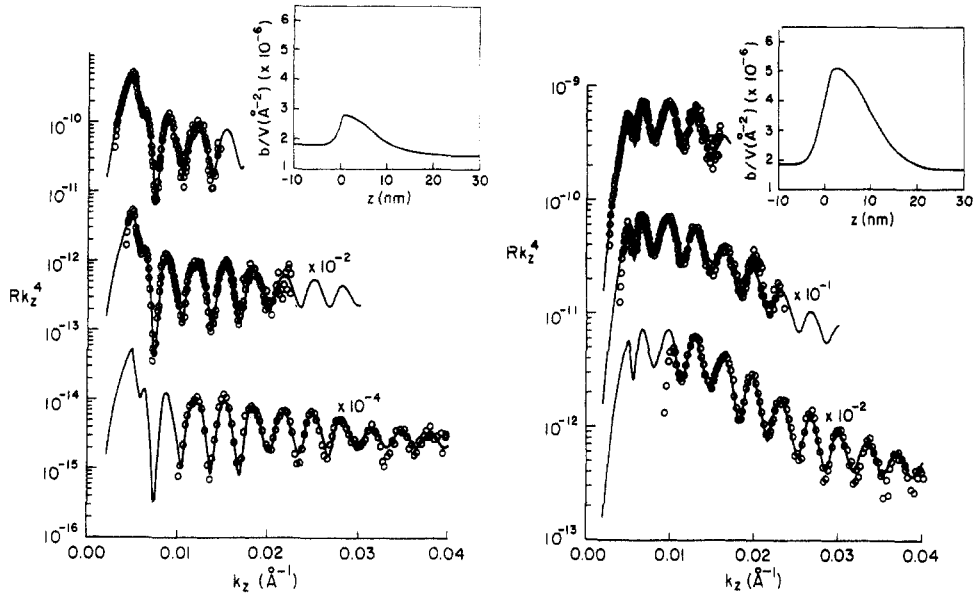

Figure 3. Neutron reflectivity data for specimens in which different quantities of the diblock copolymer are added to the PS homopolymer leading to a volume fraction ϕ_∞ of diblock copolymer in the PS phase far from the interface of (a, left) 0.004 and (b, right) 0.048; the incident angles are approximately 0.4, 0.6, and 1.4°, respectively.

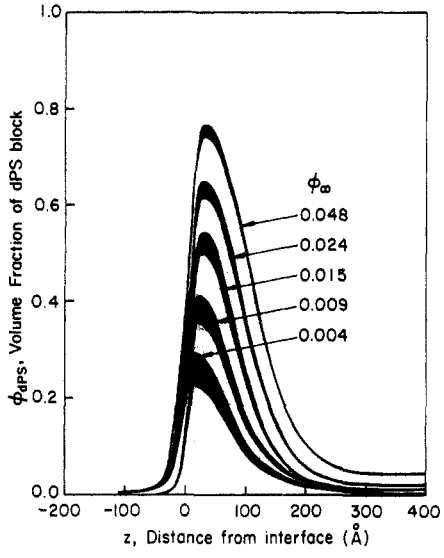

Figure 4. Volume fraction versus depth profile of dPS block in the dPS–PVP diblock copolymer, $\phi_{dPS}(z)$, converted from reflectivity data as shown in Figure 3 for various ϕ_∞'s. The thickness of the lines indicates the uncertainty accompanying the conversion.

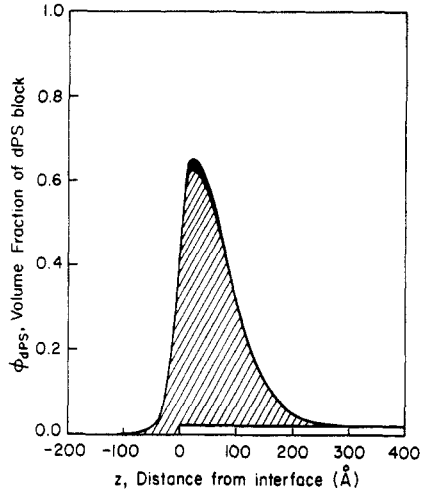

Figure 5. Volume fraction versus depth profile of dPS block in the dPS–PVP diblock copolymer, $\phi_{dPS}(z)$, for ϕ_∞ of 0.024. The cross-hatched area represents the interfacial excess z^*_{dPS} of the dPS blocks.

Reflectivity as a function of k_z was measured for the samples with ϕ_∞ of 0.004, 0.009, 0.015, 0.024, and 0.048, respectively. Examples of the reflectivity data are shown in Figure 3 to illustrate the good agreement between the reflectivity calculated from the (b/V) profiles and the measured reflectivity. Profiles of $\phi_{dPS}(z)$ for various ϕ_∞ determined from the (b/V) profiles are summarized in Figure 4. The thickness of the line is used to depict the uncertainty associated with this conversion process. It should be pointed out that while a ±10% deviation from the given ϕ_∞ may not alter the calculated reflectivity data significantly, mass conservation of the block copolymer ensures that ϕ_∞ is appropriately chosen. The interfacial excess of block copolymer z^*_i can be estimated by the following equation:

$$z^*_i = \frac{N_c}{N_{dPS}} z^*_{dPS} = \frac{N_c}{N_{dPS}} \int_{-\infty}^{\infty} (\phi_{dPS}(z) - \phi_{dPS}(\text{bulk}))\, dz \quad (5)$$

where $\phi_{dPS}(z)$ is the volume fraction of dPS block at depth z and ϕ_{dPS}(bulk) is its value in the PS homopolymer phase far from the interface after annealing. The parameters N_c and N_{dPS} are the degrees of polymerization of the block copolymer and its dPS block, respectively. An example of the $\phi_{dPS}(z)$ profile corresponding to $\phi_\infty = 0.024$ is given in Figure 5, where the shaded area represents the interfacial excess of dPS block, z^*_{dPS}. Figure 6 shows the comparison of z^*_i as a function of ϕ_∞, the so-called segregation isotherm, measured by integrating the high-resolution $\phi_{dPS}(z)$ profile from NR and the low-resolution $\phi_{dPS}(z)$ profile from FRES,[19] respectively. Good agreement is found, confirming that the procedure for converting the (b/V) profile to the $\phi_{dPS}(z)$ profile is reasonable.

The segregation isotherm may be fitted by any of the theories, the SCMF, Leibler's, or Semenov's, by treating the Flory interaction parameter χ as an adjustable parameter; χ is determined to be 0.105 from the SCMF theory, 0.07 from Leibler's theory, and 0.1 from Semenov's theory, respectively. All of the theories reproduce the segregation isotherm well at large ϕ_∞. Leibler's theory shows some deviation from the measured isotherm in the low-ϕ_∞ region[12] mainly due to the fact that Leibler's "dry

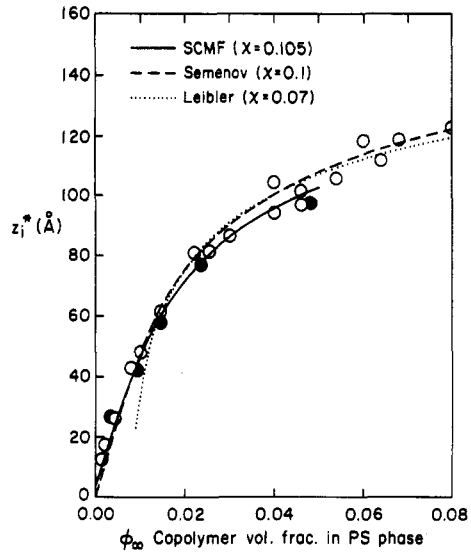

Figure 6. Segregation isotherm obtained from neutron reflectivity data (solid circles) and from forward recoil spectrometry (open circles). The fittings from the SCMF, Leibler, and Semenov theories are shown by lines: solid line, SCMF with $\chi = 0.105$; dotted line, Leibler's theory with $\chi = 0.07$; dashed line, Semenov's theory with $\chi = 0.1$.

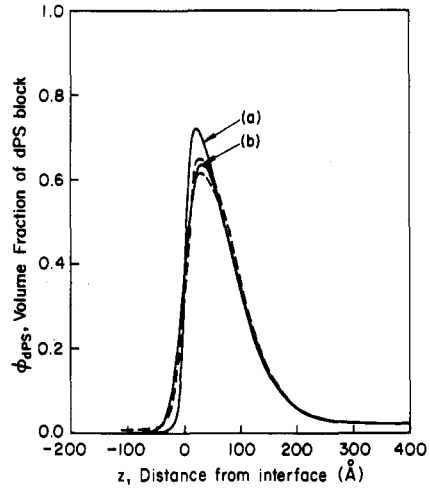

Figure 7. Volume fraction versus depth profile of dPS block in the dPS–PVP diblock copolymer, $\phi_{dPS}(z)$, for ϕ_∞ of 0.024 where the dashed lines represent the upper and lower bounds for the data. The solid line (a) represents the profile predicted by the SCMF theories; solid line (b) represents the SCMF prediction convoluted with a Gaussian with $\sigma = 18$ Å.

brush" assumption[11] is invalid in the regime of low interfacial chain density. The χ values obtained from the fit to either the SCMF or Semenov's theory for PS–PVP are consistent with the χ estimated by Shull et al.[27] from the measured heat of mixing between ethylbenzene and 2-ethylpyridine. The success of the SCMF and Semenov theories compared to the Leibler theory indicates the importance of including the entropy of localization of the copolymer joints in a theory to model the segregation.

Figure 7 shows the comparison between the dPS segment density profile predicted by the SCMF theory, using the value of χ required to fit the measured isotherm (curve a), and the measured profile for the case $\phi_\infty = 0.024$. As seen in Figure 7, the SCMF result can reproduce the $\phi_{dPS}(z)$ profile accurately except for the fact that the measured profile is broader at the interface than the predicted profile. One possibility is that the broadening may be caused by smearing due to the instrumental depth resolution. The smearing of instrumental resolution can be simulated by convoluting the predicted profile with a Gaussian function

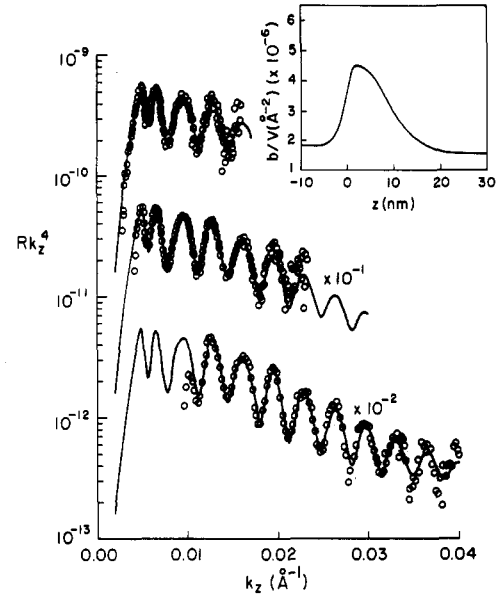

Figure 8. Fit of the SCMF theory to the neutron reflectivity data corresponding to $\phi_\infty = 0.024$; the reflectivity is calculated from a (b/V) profile (as shown in the inset) which is calculated based on the volume fraction profiles of each component obtained by applying a Gaussian convolution of $\sigma = 18$ Å to the profiles predicted by the SCMF theory.

defined as eq 6 whose full-width at half-maximum, $2(2 \ln 2)^{1/2}\sigma$, represents the instrumental depth resolution.

$$G(z) = \frac{1}{(2\pi)^{1/2}\sigma} \exp\left(-\frac{z^2}{2\sigma^2}\right) \tag{6}$$

As seen in Figure 7, the SCMF prediction falls right on the measured profile if the profile is convoluted with a Gaussian with $\sigma = 18$ Å (curve b). However, this value of σ is considerably larger than the instrumental resolution, which is <10 Å. In contrast, the Heaviside function profile assumed in Leibler's theory cannot be reconciled by applying any appropriate smearing function. Since the $\phi_{dPS}(z)$ profile predicted by Semenov's theory is not explicitly reported in his recent paper,[14] no discussion on this point will be addressed in this paper. (However, it is certainly feasible using Semenov's theory to predict the $\phi_{dPS}(z)$ profile.[28]) To demonstrate unambiguously that convoluting the SCMF profile with a Gaussian can provide a good fit to the NR data, the reflectivity is computed from a (b/V) profile derived from (via eq 4) the SCMF profile convoluted with a $G(z)$ with $\sigma = 15$ Å. The agreement between the calculated and measured NR shown in Figure 8 is excellent.

An interface which is broader than that predicted by the SCMF theory is measured for all ϕ_∞'s. Nevertheless, convoluting the SCMF prediction with $G(z)$ produces a good fit for all ϕ_∞'s as shown in Figure 9. The values of σ necessary to reproduce the broadening are summarized for all these ϕ_∞'s in Table 2. The upper and lower limits of σ correspond to the approximate maximum and minimum values of σ needed to compel the convoluted profiles lie within the limits of uncertainty of the $\phi_{dPS}(z)$ profile. The square of the additional σ required to fit the measured profile is equivalent to the smearing caused by an apparent roughness[29] at the interface with mean-square magnitude of $\langle \Delta z^2 \rangle$, i.e., $\langle \Delta z^2 \rangle = \sigma^2$. It is well known that interfacial capillary waves create undulations in liquid–vapor or liquid–liquid interfaces[30] and thus may broaden the intrinsic interfacial structure depending upon the wavelength. The roughness caused by the perturbation

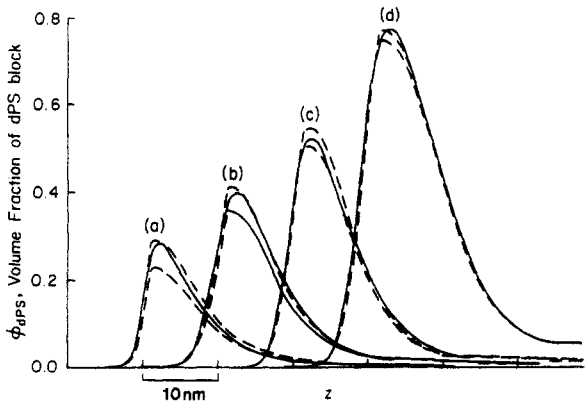

Figure 9. Volume fraction versus depth profiles of dPS block in the dPS–PVP diblock copolymer, $\phi_{dPS}(z)$, for ϕ_∞ of (a) 0.004, (b) 0.009, (c) 0.015, and (d) 0.048; the dashed lines represent the upper and lower bounds of data. The solid line represents the profile predicted by SCMF convoluted by a Gaussian function with standard deviations as follows: (a) σ = 11 Å; (b) σ = 19 Å; (c) σ = 15 Å; (d) σ = 20 Å.

Table 2. Summary of Interfacial Excess, Interfacial Tension, and the σ Parameter of the Gaussian Convolution Function as a Function of ϕ_∞

ϕ_∞	interfacial excess, z_i^* (Å)	interfacial tension, γ (dyn/cm)	σ (Å)
0		3.13[a]	8–16[b]
0.004	27 ± 4	2.87 ± 0.02	8–15
0.009	42 ± 3	2.73 ± 0.02	15–23
0.014	58 ± 3	2.61 ± 0.05	13–19
0.024	77 ± 2	2.42 ± 0.05	15–21
0.048	97 ± 2	2.09 ± 0.05	18–22

[a] Determined by the following formula:[23] $\gamma = \gamma_\infty[1 - (\pi^2/12\chi)(1/P_{hPS} + 1/P_{hPVP}) + ...]$ where γ_∞ is the interfacial tension for homopolymer of infinite molecular weight. [b] $\sigma = [(w^2 - w_{eq3}^2)/2\pi]^{1/2}$, where w_{eq3} is a w calculated from eq 3 in the text.

of the capillary wave, namely, the averaged amplitude of interfacial undulations, is proportional to the reciprocal of the interfacial tension, as expressed by eq 7.[30-32]

$$\langle \Delta z^2 \rangle = \frac{k_B T}{2\pi\gamma} \ln\left(\frac{\lambda_{max}}{\lambda_{min}}\right) \tag{7}$$

where γ is the interfacial tension. λ_{min} and λ_{max} are the lower and upper bounds of the cutoff capillary wavelength, respectively. The interfacial tension plays the role of restoring force which acts against the thermal fluctuations and leads to a finite value of $\langle \Delta z^2 \rangle$. λ_{max} can be chosen as the coherence length of the neutron beam because roughness (undulation) associated with the waves whose wavelengths exceed this coherence length of the neutron beam are scattered incoherently and thus do not contribute to the reflectivity. The coherence length, and thus λ_{max}, is estimated to be 0.025 mm in this study. The undulation of such an interface with segregated copolymer chains can be imagined as the bending of a "brush"; the wavelength associated with possible undulation modes of such an interface is therefore constrained by the stretching of the segregated copolymer chains in the brush to be a few R_g, where R_g is the radius of gyration of the copolymer. Both Semenov[31] and Shull et al.[32] use the interfacial width as an estimate of λ_{min}. Nevertheless, it should be noted that since $\ln(\lambda_{max}/\lambda_{min})$ is a weak function of $\lambda_{max}/\lambda_{min}$, the exact value of λ_{min} may not be important, and thus we take $\lambda_{min} = 2R_g$ for an estimation of eq 7. The interfacial tension listed in Table 2 is determined from the SCMF isotherm and the corresponding measured ϕ_∞ (or the corresponding z^*_i). A knowledge of ϕ_∞ and the χ parameter is sufficient for us to specify the chemical potential of the block copolymer and compute the interfacial tension γ via the Gibbs absorption equation[27] as shown below:

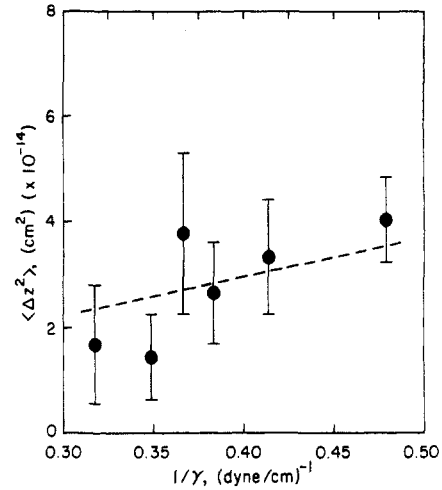

Figure 10. Apparent roughness as a function of interfacial tension. The interfacial tension is estimated using the SCMF theory for the corresponding ϕ_∞. The dashed line is predicted from eq 7 with λ_{max} = 0.025 mm and λ_{min} = 14 nm = $2R_g$.

$$\gamma = \gamma_0 - \frac{\rho}{N_c}\int_{-\infty}^{\mu} z^*_i \, d\mu \tag{8}$$

where γ_0 is the interfacial tension in the absence of copolymer; ρ is the segment density of the pure block copolymer which is approximated by its value for PS[26] of 0.0094 mol/cm^3. As seen in Figure 10, the mean-square interfacial roughness $\langle \Delta z^2 \rangle$ monotonically increases with the reciprocal of the interfacial tension. The dashed line in Figure 10 represents their relationship evaluated by eq 7, which is qualitatively consistent with the data. Therefore, we believe that the excess broadening is due to the apparent roughness caused by capillary waves on the equilibrium interface, waves whose amplitude is increased by the decrease in the interfacial tension accompanying the block copolymer segregation.

Conclusions

(1) Neutron reflectometry can be used to determine the segment density profiles of the dPS block in a dPS–PVP block copolymer segregating to the interface between PS and PVP homopolymers under conditions where the segregated "brush" is in equilibrium with free block copolymer chains with a specified chemical potential.

(2) Self-consistent mean field theory is capable of reproducing both the shape of the segregation isotherm (with a selected value of χ) and the form of the dPS block segment density profile measured by NR if the roughening of the interface by capillary waves is allowed for.

(3) The mean-square interfacial roughness $\langle \Delta z^2 \rangle$ extracted from the fitting procedures increases (with increasing ϕ_∞) with $1/\gamma$, where γ is the interfacial tension determined from the SCMF theory. This result strongly supports conclusion 2 that the interfacial roughening is due to capillary waves.

Acknowledgment. K.H.D. thanks Dow Chemical for fellowship support through the Polymer Outreach Program of the Materials Science Center (MSC), and L.J.N. acknowledges the polymer fellowship from the Department of Education. The experimental work is supported by the MSC, which is funded by the MRL Program of the National Science Foundation under Award No. DMR-9121654, and by IPNS at Argonne National Laboratory,

which is funded by the U.S. Department of Energy under Contract W-31-109-ENG-38. The assistance of Nancy Stoffel and Bill Dozier with NR is greatly appreciated. We also benefited from using the National Nanofabrication Facility at Cornell University, which is funded by the NSF.

Appendix: Conversion of the (b/V) Profile to the ϕ_{dPS} Profile

The scattering length density profile is divided into five regions. The conversion to volume fraction profile for each region is discussed below.

(1) In the PS Host Phase Far from the Interface. In the PS host phase far from the interface, polymer components are intimately mixed and thus uniformly distributed. Therefore the volume fraction of each block can be expressed as

$$\phi_{dPS} = \phi_\infty \frac{N_{dPS}}{N_c} \qquad \phi_{PVP} = \phi_\infty \frac{N_{PVP}}{N_c} \tag{A1}$$

where $N_c = N_{dPS} + N_{PVP}$. In addition, for these strongly immiscible polymers, the amount of PVP homopolymer dissolved in the PS bulk phase is negligible, and thus

$$\phi_{hPS} \cong 1 - \phi_\infty \qquad \phi_{hPVP} \cong 0 \tag{A2}$$

By substituting eqs A1 and A2 into eq 4, one can solve for ϕ_∞, which can be written as

$$\phi_\infty = \frac{\left(\frac{b}{V}\right)_{bulk} - \left(\frac{b}{V}\right)_{hPS}}{\frac{N_{dPS}}{N_c}\left(\frac{b}{V}\right)_{dPS} - \frac{N_{PVP}}{N_c}\left(\frac{b}{V}\right)_{PVP} - \left(\frac{b}{V}\right)_{hPS}} \tag{A3}$$

where $(b/V)_{bulk}$ is the value of $(b/V)_{total}$ in the PS homopolymer host phase.

(2) In the PVP Bulk Phase Far from the Interface. The volume fraction of copolymer in the PVP bulk phase is proportional to $\exp(-\chi N_{dPS})$. Since $N_{dPS} = 597$, this volume fraction is negligible. The volume fraction of hPS in the PVP phase is also negligible due to the large value of P_{PS}.

(3) At the Position Corresponding to the Maximum Scattering Length Density. Based on the fact that the difference of neutron scattering length density between hPS and PVP is significantly less than the scattering length density of dPS, one can replace $(b/V)_{PVP}$ and $(b/V)_{hPS}$ with a common $(b/V)_i$ (either $(b/V)_{PVP}$ or $(b/V)_{hPS}$) to solve for the volume fraction of the dPS block at the position corresponding to the maximum of the measured (b/V) profile; viz.

$$\phi_{dPS,max} = \frac{\left(\frac{b}{V}\right)_{max} - \left(\frac{b}{V}\right)_i}{\left(\frac{b}{V}\right)_{dPS} - \left(\frac{b}{V}\right)_i} \tag{A4}$$

where i = PVP (lower bound) or hPS (upper bound). This result provides us with the lower and upper bounds of the maximum dPS volume fraction.

(4) In the Vicinity of the Interface on the Side of the PS Host Phase. Equation 4 can be rearranged as written below to solve for $\phi_{dPS}(z)$.

$$\phi_{dPS}(z) = \frac{\left[\left(\frac{b}{V}\right)_z - \left(\frac{b}{V}\right)_{PVP}\right] + \phi_{hPS}(z)\left[\left(\frac{b}{V}\right)_{PVP} - \left(\frac{b}{V}\right)_{hPS}\right]}{\left(\frac{b}{V}\right)_{dPS} - \left(\frac{b}{V}\right)_{PVP}} \tag{A5}$$

As seen, $\phi_{hPS}(z)$ has to be known to estimate $\phi_{dPS}(z)$. Since $\phi_{hPS}(z)$ asymptotically approaches two boundary values corresponding to $(b/V)_{bulk}$ and $(b/V)_{max}$ (as indicated by eq A6), $\phi_{hPS}(z)$ may be described by a functional interpolation between these two asymptotic limits.

$$\phi_{hPS}(\text{bulk}) = 1 - \phi_\infty$$

$$0 \le \phi_{hPS}(z@(b/V)_{max}) \le \phi'_{PS} \tag{A6}$$

The uncertainty of $\phi_{hPS}(z@(b/V)_{max})$ is a result of the arbitrary choice of $(b/V)_i$ in eq A4, and thus ϕ'_{dPS} can be calculated by equating eq A4 = eq A5 with i = hPS. Since the scattering length density of dPS is much higher than that of the rest of the components and the copolymer has only a short PVP block, the functional form for interpolation can be reasonably assumed to have the same decay shape of the measured scattering length density profile from the peak to the PS bulk phase, as described by eq A7.

$$\frac{\phi_{hPS}(z) - \phi_{hPS}(z@(b/V)_{max})}{\phi_{hPS}(\text{bulk}) - \phi_{hPS}(z@(b/V)_{max})} = \frac{\left(\frac{b}{V}\right)_{max} - \left(\frac{b}{V}\right)_z}{\left(\frac{b}{V}\right)_{max} - \left(\frac{b}{V}\right)_{bulk}} \tag{A7}$$

Then eq A5 is used to estimate $\phi_{dPS}(z)$ near the interface approached from the PS side.

(5) In the Vicinity of the Interface on the Side of the PVP Phase. Similar treatments as described in the previous paragraph are applied to estimate $\phi_{dPS}(z)$ in this section on the PVP side of the interface. By rearranging eq 4, we can write $\phi_{dPS}(z)$ as

$$\phi_{dPS}(z) = \left\{\left[\left(\frac{b}{V}\right)_z - \left(\frac{b}{V}\right)_{hPS}\right] - (\phi_{PVP}(z) - \phi_{hPVP}(z))\left[\left(\frac{b}{V}\right)_{PVP} - \left(\frac{b}{V}\right)_{hPS}\right]\right\} \Big/ \left\{\left(\frac{b}{V}\right)_{dPS} - \left(\frac{b}{V}\right)_{hPS}\right\} \tag{A8}$$

Again, as seen, $\phi_{PVP}(z) + \phi_{hPVP}(z)$ has to be known to estimate $\phi_{dPS}(z)$. Two asymptotic values of $\phi_{PVP}(z) + \phi_{hPVP}(z)$ can be found by similar arguments used to obtain eq A6:

$$\phi_{PVP}(\text{hPVP phase}) + \phi_{hPVP}(\text{hPVP phase}) = 1$$

$$0 \le \phi_{PVP}(z@(b/V)_{max}) + \phi_{hPVP}(z@(b/V)_{max}) \le \phi'_{PVP} \tag{A9}$$

where ϕ'_{PVP} can be estimated by equating eq A4 = eq A8 with i = PVP. The functional form chosen for the interpolation to estimate $\phi_{PVP}(z) + \phi_{hPVP}(z)$ is

$$\frac{1 - [\phi_{PVP}(z) + \phi_{hPVP}(z)]}{1 - [\phi_{PVP}(z@(b/V)_{max}) + \phi_{hPVP}(z@(b/V)_{max})]} = \frac{\left(\frac{b}{V}\right)_z - \left(\frac{b}{V}\right)_{PVP}}{\left(\frac{b}{V}\right)_{max} - \left(\frac{b}{V}\right)_{PVP}} \tag{A10}$$

and eq A8 is then used to solve for $\phi_{dPS}(z)$ near the interface approaching from the PVP side.

References and Notes

(1) Kulich, D. M.; Kelley, P. D.; Pace, J. E. *Encyclopedia of Polymer Science and Engineering*, 2nd ed.; Mark, H. F., Bikales, N. M., Overberger, C. G., Menges, G., Kroschwitz, J. I., Eds.; John Wiley & Sons: New York, 1985; Vol. I, p 388.
(2) Brown, H. R. *Macromolecules* **1989**, *22*, 2859.
(3) Creton, C.; Kramer, E. J.; Hadziioannou, G. *Macromolecules* **1991**, *24*, 1846.
(4) Washiyama, J.; Creton, C.; Kramer, E. J. *Macromolecules* **1992**, *25*, 4751.
(5) Willett, J. L.; Wool, R. P. *Macromolecules* **1993**, *26*, 5336.
(6) Anastasiadis, S. H.; Gancarz, I.; Koberstein, J. T. *Macromolecules* **1988**, *21*, 2980.
(7) Fayt, R.; Jérôme, R.; Teyssié, Ph. *Makromol. Chem.* **1986**, *187*, 837.
(8) Ouhadi, R.; Fayt, R.; Jérôme, R.; Teyssié, Ph. *Polym. Commun.* **1986**, *27*, 212.
(9) Heikens, D.; Barentsen, W. M. *Polymer* **1977**, *18*, 70.
(10) Russell, T. P. *Mater. Sci. Rep.* **1990**, *5*, 171.
(11) Leibler, L. *Makromol. Chem., Macromol. Symp.* **1988**, *16*, 1.
(12) Dai, K. H.; Kramer, E. J.; Shull, K. R. *Macromolecules* **1992**, *25*, 220.
(13) Green, P. F.; Russell, T. P. *Macromolecules* **1991**, *24*, 2931.
(14) Semenov, A. N. *Macromolecules* **1992**, *25*, 4967.
(15) (a) Helfand, E.; Tagami, Y. *Polym. Lett.* **1971**, *9*, 741. (b) Helfand, E.; Tagami, Y. *J. Chem. Phys.* **1972**, *56*, 3592.
(16) Noolandi, J.; Hong, K. M. *Macromolecules* **1982**, *15*, 482.
(17) Noolandi, J. *Makromol. Chem., Rapid Commun.* **1991**, *12*, 517.
(18) Shull, K. R.; Kramer, E. J. *Macromolecules* **1991**, *23*, 4769.
(19) Russell, T. P.; Anastasiadis, S. H.; Menelle, A.; Felcher, G. P.; Satija, S. K. *Macromolecules* **1991**, *24*, 1575.
(20) For the details of the surface preparation of silicon, please see: Frantz, P.; Granick, S. *Langmuir* **1992**, *8*, 1176.
(21) Dai, K. H.; Kramer, E. J. *Polymer* **1994**, *35*, 157.
(22) Born, M.; Wolf, E. *Principles of Optics*; Pergamon Press: Oxford, 1975.
(23) Jones, R. A. L.; Norton, L. J.; Kramer, E. J.; Composto, R. J.; Stein, R. S.; Russell, T. P.; Mansour, A.; Karim, A.; Felcher, G. P.; Rafailovich, M. H.; Sokolov, J.; Schwarz, S. A. *Europhys. Lett.* **1990**, *12*, 41.
(24) Helfand, E.; Tagami, Y. *J. Polym. Sci.* **1971**, *B9*, 741.
(25) Broseta, D.; Fredrickson, G. H.; Helfand, E.; Leibler, L. *Macromolecules* **1990**, *23*, 132.
(26) Tangari, C.; King, J. S.; Summerfield, G. C. *Macromolecules* **1982**, *15*, 132.
(27) Shull, K. R.; Kramer, E. J.; Hadziioannou, G.; Tang, W. *Macromolecules* **1990**, *23*, 4780.
(28) Semenov, A. N., private communication.
(29) It should be noted that $w = (2\pi)^{1/2}\sigma$, with w and σ defined in eqs 2 and 6, respectively.
(30) Croxton, C. A. *Statistical Mechanics of the Liquid Surface*; John Wiley & Sons: New York, 1980.
(31) Semenov, A. N. *Macromolecules* **1993**, *26*, 6617.
(32) Shull, K. R.; Mayes, A. M.; Russell, T. P. *Macromolecules* **1993**, *26*, 3929.